0 0 0 0 4 2 0 3 2 9 4

Submitted to Journal of Chemical Physics

RECEIVED
BERKELEY LABORATORY

JUL 18 1975

LIBRARY AND
DOCUMENTS SECTION

LBL-3494
Preprint c.1

RELATIVISTIC AND CORRELATION EFFECTS IN THE 21.2-eV PHOTOEMISSION SPECTRUM OF ATOMIC LEAD

S. Süzer, M. S. Banna, and D. A. Shirley

April 1975

Prepared for the U. S. Energy Research and
Development Administration under Contract W-7405-ENG-48

For Reference

Not to be taken from this room

LAWRENCE BERKELEY LABORATORY
UNIVERSITY OF CALIFORNIA
BERKELEY

LBL-3494
c.1

DISCLAIMER

This document was prepared as an account of work sponsored by the United States Government. While this document is believed to contain correct information, neither the United States Government nor any agency thereof, nor the Regents of the University of California, nor any of their employees, makes any warranty, express or implied, or assumes any legal responsibility for the accuracy, completeness, or usefulness of any information, apparatus, product, or process disclosed, or represents that its use would not infringe privately owned rights. Reference herein to any specific commercial product, process, or service by its trade name, trademark, manufacturer, or otherwise, does not necessarily constitute or imply its endorsement, recommendation, or favoring by the United States Government or any agency thereof, or the Regents of the University of California. The views and opinions of authors expressed herein do not necessarily state or reflect those of the United States Government or any agency thereof or the Regents of the University of California.

0 0 0 0 4 2 0 6 2 9 5

LBL-3494

RELATIVISTIC AND CORRELATION EFFECTS IN THE 21.2-eV PHOTOEMISSION SPECTRUM OF ATOMIC LEAD *

S. Süzer, M. S. Banna, and D. A. Shirley

Department of Chemistry and
Lawrence Berkeley Laboratory, University of California
Berkeley, California 94720

ABSTRACT: Photoelectron spectra were obtained for atomic lead in the 700-800°C range, using HeI radiation (21.2 eV) and a special, high-temperature cell. Relativistic effects were obvious, most notably in the relative intensity of 1.000:0.071 in the peaks arising from $Pb^+(s^2p;\ ^2P_{1/2})$: $Pb^+(s^2p;\ ^2P_{3/2})$ states. This is a consequence of the $Pb(s^2p^2;\ ^3P_0)$ ground state being in fact mostly $s^2p_{1/2}{}^2$. Correlation effects were also apparent. Several final states inaccessible from an s^2p^2 initial-state configurations were reached; this was explained by admixtures of the configurations sp^2 and s^2d^2 into the initial state. All transitions that would be allowed by the presence of these peaks were actually found. These "direct" observations of configuration interaction give an operational meaning to this concept that is not available to most spectroscopic methods. Energy-loss peaks were observed at higher pressure and attributed to excitation of optical levels in neutral Pb by photoelectrons.

I. INTRODUCTION

This is the second in a series of papers reporting photoelectron spectroscopic studies of atomic species in the gas phase, using samples heated to high temperatures. In the first paper[1], on atomic cadmium, we reported the observation of initial-state configuration interaction (ISCI). This paper is addressed to atomic lead.

When an N-electron system absorbs a photon, the process is usually constrained to obey electric dipole selection rules. This constraint is often quite restrictive for ordinary absorption spectroscopic experiments in which the N electrons are all bound in the final state. For photoelectron spectroscopic transitions, of the form

$$N \rightarrow (N - 1)^{+} + e^{-} \tag{1}$$

however, any state of the N-1 electron system can in principle be reached if dipole selection rules can be satisfied for the overall system, with the continuum state of the photoelectron included. This substantially removes the restrictions imposed by the dipole selection rule, and the strongest remaining selection rule is that the transition must be accessible via one-electron operators.

Two important implications follow directly. First, most or all of the electronic states of the N-1 electron system that are reached by one-electron operators will appear in the photoelectron spectrum. The electron kinetic energies yield the level energies directly. Thus a more or less complete array of final states is obtained, with each at its correct energy.

Second, correlation effects, as manifested through configuration interaction, can be observed directly. This follows because those eigenstates of the (final) N-1 electron system possessing a given symmetry are described as admixtures of the nominal N-1 electron configurations of that symmetry. Thus each eigenstate may consist in part of the nominal lowest-energy N-1 electron configuration, and may be directly accessible by photoemission from the ground state. In addition, the ground state itself may be comprised of several admixed configurations, allowing transitions to states that would not be reached if only the dominant configuration were present. This latter effect is in fact the important one in the systems that have been studied to date. In neutral cadmium[1] and mercury[2], for example, admixtures of the configuration $(np^2;{}^1S)$ into the nominal ground-state configuration $(ns^2;{}^1S)$ allows the $[np;\ {}^2P_{1/2}]$ and $[np;\ {}^2P_{3/2}]$ final states to be reached.

Group IV elements, with a nominal s^2p^2 ground-state configuration, present an important series that has received considerable theoretical attention. In carbon, the first member of the series, Bagus et al.[3-5] have shown that explicit correlation effects must be introduced to account for the observed ${}^3P, {}^1D, {}^1S$ multiplet separations as well as their ratios $({}^3P - {}^1D)/({}^3P - {}^1S)$. In lead, the last member, these effects are expected to be similar magnitude, and relativistic effects should be important as well.[6]

In this paper we report the observation of correlation and relativistic effects on the HeI photoionization spectrum of Pb vapor. Experimental details are given in Section II and results in Section III.

Relativistic and correlation effects are discussed in Section IV. Section V deals with the inelastic loss spectrum. Conclusions are given in Section VI.

II. EXPERIMENTAL

The experiments were carried out in a Perkin-Elmer PS-18 photoelectron spectrometer modified for high-temperature work. The modifications included a boron nitride oven surrounding the tantalum ionization chamber and the sample compartment. Essential components are shown in Fig. 1. The oven is capable of reaching temperatures up to 1000°C.

The temperature was monitored, on top of the sample compartment outside the vacuum chamber, by a thermocouple which reads approximately 15-25°C lower than the temperature in the ionization chamber. The gas pressure was not measured directly, but the optimum operating temperature was determined for a count rate of $2\text{-}4 \times 10^3$ counts/sec on the most intense peak. Then the same spectra were taken at temperatures of ± 30°C from the optimum to differentiate between the inelastic loss peaks and the real photoionization peaks. Energy calibration was done by introducing Ar and Xe together with the sample in a separate run. Resolutions of less than 50 mV (FWHM) on the Ar peaks have been achieved. Although the instrument is capable of better resolution, local non-uniform micropotentials, due to charging on the surfaces of the ionization chamber, invariably broaden the lines. A heating current of 1.5 amp, necessary to obtain 800°C, was not observed to give any extra broadening.

The aforementioned charging was also observed to affect the relative intensity of the peaks. Relative intensities were found to depend also on the degree of inelastic scattering of electrons due to a finite sample pressure.[7,8] The reported area ratios were corrected for the change of the spectrometer transmission with electron kinetic energy ($\Delta E/E$ = constant).

Data were collected and stored in a multi-channel analyzer (1024, 2048 or 4096 channels). The digitally controlled supply, which provided voltages to the spectrometer analyzer plates, also provided signals to the MCA. This setup enabled us to accumulate the data over many scans. Typically 100-200 scans were taken for for each spectrum, over 2-4 hours

III. RESULTS

The He I photoelectron spectrum of Pb at 715°C is shown in Fig. 2. Assignments of the peaks were made by comparison of their binding energies with optical data.[9] These assignments and derived parameters are shown in Table I.

The spectra from atomic Pb($6s^2 6p^2; {}^3P_0$) is expected to show four peaks at binding energies 7.415 eV, 9.160 eV, 14.593 eV, and 18.353 eV, arising respectively from transitions to the ($6s^2 6p; {}^2P_{1/2}$), ($6s^2 6p; {}^2P_{3/2}$), ($6s6p^2; {}^4P_{1/2}$), and ($6s6p^2; {}^2P_{1/2}$) final states of Pb^+. In addition to these four lines, we have also observed four weaker peaks at 15.61 eV, 15.96 eV, 16.06 eV, and 16.58 eV binding energies, corresponding respectively to the ($6s6p^2; {}^4P_{3/2}$) ($6s^2 6d; {}^2D_{5/2}$), ($6s^2 6d; {}^2D_{3/2}$) and ($6s6p^2; {}^4P_{5/2}$) final states. Also, three more peaks show up in the spectrum. The peaks designated in the

figure by HI and OI are assigned to impurity lines; i.e., photoionization of Pb to the $Pb^+(^2P_{1/2})$ line at 7.4 eV through excitation by the resonant radiation from the impurities HI and OI (atomic hydrogen and oxygen). The peak at 9.85 eV can be identified neither with any known transition nor as any sample impurity, and we tentatively assign it as arising from Pb_2 molecular photoionization.

The first unusual feature noticed in the spectrum is the inversion of the intensities of $(s^2p;^2P_{1/2})$ and $(s^2p;^2P_{3/2})$, with the former dominant. This is explained in Section IVA. It is a consequence of relativistic effects (j-j coupling).

A second feature is the presence of the aforementioned four extra peaks. These are attributed to the correlation effects, as discussed in Section IVB.

Finally, in going to higher temperatures, we see new peaks arising from inelastic losses. In Section V we present the spectrum and discuss the nature of these transitions.

IV. DISCUSSION

A. Relativistic Effects

Spin-orbit coupling splits the 6p shell into $p_{1/2}$ and $p_{3/2}$ subshells, with the former being lower in energy. For the two-electron case we have three configurations; $(p_{1/2})^2$, $(p_{1/2}p_{3/2})$ and $(p_{3/2})^2$. The ground state of p^2 (J = 0) can, in general, be written in terms of j-j coupled states as

$$\Psi = c_1 \, (p_{1/2})^2 + c_2 \, (p_{3/2})^2 .$$

In terms of L.S coupled states this corresponds to a mixture of $^3P_0$ and $^1S_0$ states. The relative weights of the two configurations will depend on the strength of the spin-orbit coupling. Relativistic Hartree-Fock (RHF) calculations[6] predict the ratio $(c_1/c_2)^2 = .081$, showing that j-j coupling is a better approximation for Pb than is L-S coupling, which gives the ratio as 0.5.

Photoionization from the outer 6p subshells yields $^2P_{1/2}$ and $^2P_{3/2}$ states of Pb^+ $(6s^26p)$, corresponding to the removal of an electron from $6p_{1/2}$ or $6p_{3/2}$ subshells,respectively. Hence the intensities of the observed lines give a measure of the relative weights of these subshells in the ground state. From Table I, our experimental intensity ratio is .071, in very good agreement with the RHF prediction. However one would have to correct for any differences in the photoionization cross sections before a final comparison could be made. The photoionization cross sections may be considerably different for each individual subshell, because the radial functions are different (RHF calculations for the mean values of $\langle r \rangle$ give respectively 3.07 and 3.52 atomic units for the $6p_{1/2}$ and $6p_{3/2}$ subshell,[6] compared to the non-relativistic value[10] of 3.46). Also, the RHF calculation did not include some correlation effects that we will show to be important, which again may affect the calculated intensity ratio.

Removal of an s electron from $(s^2p^2;\ ^3P_0)$ gives $^4P_{1/2}$ and $^2P_{1/2}$ (sp^2) lines. But for Pb^+, $(6s\ 6p^2;\ ^4P_{1/2})$ corresponds to $6s(6p_{1/2})^2$ and $^2P_{1/2}$ corresponds to $6s(6p_{1/2}\ 6p_{3/2})$ in j-j coupling. On this argument alone we would expect to see an intense $^4P_{1/2}$ line and a relatively weak $^2P_{1/2}$ line, but from Table I the relative intensities are .075 and .110,

respectively. While the cross sections may be somewhat different for these two processes, we believe that the main reason for the $^2P_{1/2}$ intensity being so high is configuration interaction in the final state. A discussion of correlation effects is given below.

B. Correlation Effects

Final-state correlation effects have been reported in the photoemission spectra from noble gases,[11] molecules[12], and solids[13]. Berkowitz, et al.[8] reported that the quasi-degenerate $6p^2$ configuration mixed into $6s^2$ in the ground state of Hg, giving satellites in the He I photoemission spectrum of atomic Hg, and we reported a similar result for Cd[1].

In open-shell atoms or molecules, the quasi-degenerate configurations are known to mix strongly with the ground state. This effect was termed "internal correlation" by McKoy and Sinanōglu.[14] For the $6s^26p^2$ ground-state configuration of Pb, $6p^4$ is perhaps the conventional configuration to be admixed, but Desclaux[6] found this mixing to be very small, because it involves promotion of two 6s electrons into the energetically unfavorable $6p_{3/2}$ subshell. Bagus et al.[3-5] reported configurations of the type $2s2p^23d$ to mix substantially into the ground state of carbon ($2s^22p^2$), although the 3d shell is not quasi-degenerate with 2p. But in Pb, the 6d shell lies very close in energy to 6p, and it is of course quasi-degenerate. Hence we expect 6d mixing to be important in the ground-state of Pb. Because the spin-orbit coupling constant is small both the $6d_{3/2}$ and $6d_{5/2}$ subshells are expected to contribute.

In Table II, we give the configurations expected to mix strongly with $6s^2 6p^2$, their final states upon photoionization, and their spectroscopic designations. We used the j-j coupling scheme and coupled the two p electrons (or two s-electrons) to the remaining two electrons to get the J = 0 initial state. We have listed only the final states which can be reached by (21.2 eV) He I radiation (these states can all be all be regarded as resulting from the ionization of a 6d electron, in an approximate description).

From Tables I and II one can see that configurations I.A would give $^4P_{3/2}$, which is observed to be 0.024 the intensity of the main line; I.B and I.C would give $^4P_{5/2}$, also observed, in intensity 0.040; I·D and I.E would give $^2D_{5/2}$ and $^2D_{3/2}$ derived from the s^2d configuration, again observed, with intensities of 0.022 and 0.019. Configurations II.F and II·G would give $^2D_{5/2}$ and $^2D_{3/2}$ derived from the configuration sp^2. These were not observed to be present. This is easily understood, because they can mix directly only with the $(6s_{1/2})^2 (6p_{3/2})^2$ part of the ground state (they would involve three-electron excitation from the $(6s_{1/2})^2(6p_{1/2})^2$ configuration and would therefore be expected to mix negligibly into this configuration).

Mixing of $6s^2 6d^2$ and $6s6p^2 6d$ configurations into the ground state of Pb can thus totally account for the presence of the satellites observed in this experiment. However it would be necessary to consider the mixing among final states as well as variations in photoionization cross-section before definite mixing coefficients could be derived from these experimental peak intensities. We are presently investigating techniques by which such quantitative comparisons with theory might feasibly be made.

Another mechanism has been suggested to account for the satellite structure, namely "conjugate shake-up"[2], in which the angular momentum of the radiation field is transferred to one of the passive electrons (i.e., the electron makes a transition to an empty orbital with higher ℓ quantum number). We can write this process for Pb as follows:

Main process: $(6s_{1/2})^2(6p_{1/2})^2 + h\nu \rightarrow [(6s_{1/2})^2\ 6p_{1/2}]^2P_{1/2} + \varepsilon d$ or εs

Conjugate shake up: $(6s_{1/2})^2(6p_{1/2})^2 + h\nu \rightarrow [(6s_{1/2})^2\ 6d_{3/2}]_{J=3/2} + \varepsilon p$

or

$$(6s_{1/2})^2(6p_{1/2})^2 + h\nu \rightarrow [6s_{1/2})(6p_{1/2})(6p_{1/2})]_{J=1/2} + \varepsilon p$$

and

$$(6s_{1/2})^2(6p_{1/2})^2 + h\nu \rightarrow [6s_{1/2})(6p_{1/2})(6p_{3/2})]_{J=3/2} + \varepsilon p.$$

Since $\Delta J = 0, \pm 1$ selection rules are operative, only $(sp^2;{}^4P_{3/2})$ and $(s^2d;{}^2D_{3/2})$ lines would be expected to be present in the spectrum. The $(sp^2;{}^4P_{5/2})$ and $(s^2d;{}^2D_{5/2})$ lines could only result from the $(6p_{3/2})^2$ part of the ground state, and would be extremely weak if not absent. Hence we believe this mechanism does not contribute much to the observed intensity of the four satellite lines. The theoretical situation as to the importance of the conjugate shake-up mechanism is unclear. Detailed calculations have shown that this mechanism is very weak for He[15], although Berkowitz et al.[2] made estimates that suggested it could be as strong as the CI mechanism in mercury.

V. INELASTIC LOSS SPECTRA

When the Pb spectrum is taken at 765°C several strong inelastic loss peaks appear. Figure 3 shows the spectrum and Table III summarizes the results. All the observed five peaks are interpreted to result from electron impact excitation of neutral Pb by photoelectrons emitted in exciting the $^2P_{1/2}$ line, at a kinetic energy of 13.80(1) eV.

Lines 1 and 2 correspond to excitation of a $6p_{1/2}$ electron into the $6p_{3/2}$ subshell, with final states $^3P_1$ and $^3P_2$. Intensities are in a ratio of ~ 1:4 which clearly deviates from the statistical ratio of 3:5. The final state $^1D_2$, 2.66 eV away, corresponding to a $(6p_{3/2})^2$ configuration is not observed, which again is a consequence of strong j-j coupling. Lines 3 and 4 are the results of excitation from 6p to 7s and 6d shells. Line 5 cannot be identified by any known transition, and we tentatively assign it to an excitation from the 6s to the 6p shell. The breadth of this line indicates more than one final state, or perhaps that the excitation takes place in Pb_2.

VI. CONCLUSIONS

This work has demonstrated the feasibility of obtaining photoemission spectra of atomic Pb at temperatures of 700-800 C, with good resolution and signal/noise ratios. The spectra showed in a very direct way—through dramatic intensity ratios or the existence of satellite lines—that relativistic and correlation effects are indeed present in the $6s^26p^2$ ground-state configuration of lead. This may be contrasted with the

relatively indirect nature of most spectroscopic methods for studying these effects. Further theoretical developments are necessary before a really quantitative interpretation of these peak intensities will be possible. With these developments, we believe that photoemission studies of this nature will be able to bring more operational meaning to the concept of configuration interaction.

REFERENCES

*Work performed under the auspices of the U. S. Energy Research and Development Administration.

1. S. Süzer and D. A. Shirley, J. Chem. Phys. 61, 2481 (1974).
2. J. Berkowitz, J. L. Dehmer, Y. K. Kim, and J. P. Desclaux, J. Chem. Phys. 61, 2556 (1974).
3. P. S. Bagus and C. M. Moser, Phys. Rev. 167, 13 (1968).
4. P. S. Bagus, N. Bessis, and C. M. Moser, Phys. Rev. 179, 39 (1969).
5. P. S. Bagus and C. M. Moser, J. Phys. B 2, 1214 (1969).
6. J. P. Desclaux, Int. J. Quan. Chem. 6, 25 (1972).
7. J. L. Dehmer and J. Berkowitz, Phys. Rev. A10, 484 (1974).
8. J. L. Gardner and J. A. R. Samson, J. Elec. Spect. 6, 53 (1975).
9. C. E. Moore, Natl. Bur. Std. (U.S.) Circ. 467, Vol. 3 (1962).
10. J. B. Mann, Los Alamos Scientific Report LA 3691 (1968).
11. D. P. Spears, H. J. Fischeck, and T. A. Carlson, Phys. Rev. A 9, 1603 (1974); F. Wuilleumier, and M. O. Krause, Phys. Rev. A 10, 242 (1974).
12. R. N. Dixon and S. E. Hull, Chem. Phys. Letters 3, 367 (1969); Michio Okuda and Neville Jonathan, J. Elec. Spect. 3, 19 (1974); A. W. Potts and T. A. Williams, J. Elec. Spect. 3, 5 (1974); J. C. Lorquet and C. Cadet, Chem. Phys. Letters 3, 198 (1970).
13. S. P. Kowalczyk, L. Ley, R. A. Pollak, F. R. McFeely, and D. A. Shirley, Phys. Rev. B7, 4009 (1973); C. S. Fadley, D. A. Shirley, A. J. Freeman, P. S. Bagus, and J. R. Mallow, Phys. Rev. Letters 23, 1397 (1969); A. Rosencwaig, H. K. Wertheim, and H. J. Guggenheim, Phys. Rev. Lett. 27, 479 (1971)
14. V. McKoy and O. Sinanoglu, J. Chem. Phys. 41, 2689 (1964).
15. R. L. Brown, Phys. Rev. A1, 341 (1970).

Table I. States of Pb^+ observed in photoemission from Pb Vapor.

Final	States	Relative intensity[a]	Binding energy, eV[b]	Energy from optical data, eV[c]
$6s^26p$	$^2P_{1/2}$	1.000	7.42(1)	7.415
	$^2P_{3/2}$	.071 (5)	9.16(1)	9.160
$6s6p^2$	$^4P_{1/2}$	.075 (5)	14.59(1)	14.593
	$^4P_{3/2}$	.024 (5)	15.61(1)	15.611
	$^4P_{5/2}$	.040 (5)	16.57(1)	16.576
$6s6p^2$	$^2P_{1/2}$	.110 (5)	18.35(1)	18.353
$6s^26d$	$^2D_{5/2}$	.022 (5)	15.97(1)	15.963
	$^2D_{3/2}$	.019 (5)	16.06(1)	16.059
$Pb_2^{+(d)}$		.014 (5)	9.85(1)	---

[a]Relative areas divided by their kinetic energies to correct for the spectrometer efficiency.

[b]This work. Values given are averages of three runs. Errors in last place are given parenthetically. The Xe lines at 12.130 eV and 13.436 eV and the Ar lines at 15.759 eV and 15.937 eV are used for calibration.

[c]Ref. 9.

[d]Assignment is tentative.

Table II. Configuration which can mix with the ground state of Pb and their final ionic states of Pb^+ excluding the $^2P_{1/2}$ and $^2P_{3/2}$ states of s^2p.

	Initial state of Pb	Final state of Pb^+	J	Spec. desig.[a]	Binding[a] energy, eV	Remarks
I.	$(6s_{1/2})^2_{J=0}\ (6p_{1/2})^2_{J=0}$	$6s_{1/2}\ (6p_{1/2})^2_{J=0}$	1/2	sp^2 $^4P_{1/2}$	14.593	Main line
II.	$(6s_{1/2})^2_{J=0}\ (6p_{3/2})^2_{J=0}$	$6s_{1/2}\ (6p_{3/2})^2_{J=0}$	1/2	sp^2 $^2S_{1/2}$	20.343	Not observed
I.A	$(6p_{1/2}6p_{3/2})_{J=1}\ (6s_{1/2}6d_{3/2})_{J=1}$	$6s_{1/2}\ (6p_{1/2}\ 6p_{3/2})_{J=1}$	3/2	sp^2 $^4P_{3/2}$	15.611	Observed
			1/2	sp^2 $^2P_{1/2}$	18.353	Observed[b]
I.B	$(6p_{1/2}\ 6p_{3/2})_{J=2}(6s_{1/2}6d_{3/2})_{J=2}$	$6s_{1/2}\ (6p_{1/2}\ 6p_{3/2})_{J=2}$	5/2	sp^2 $^4P_{5/2}$	16.576	Observed
I.C	$(6p_{1/2}\ 6p_{3/2})_{J=2}(6s_{1/2}\ 6d_{5/2})_{J=2}$		3/2	sp^2 $^4P_{3/2}$	20.389	Not observed
I.D	$(6s_{1/2})^2_{J=0}\ (6d_{3/2})^2_{J=0}$	$(6s_{1/2})^2_{J=0}\ 6d_{3/2}$	3/2	s^2d $^2D_{3/2}$	16.059	Observed
I.E	$(6s_{1/2})^2_{J=0}\ (6d_{5/2})^2_{J=0}$	$(6s_{1/2})^2_{J=0}\ 6d_{5/2}$	5/2	s^2d $^2D_{5/2}$	15.963	Observed
II.F	$(6p_{3/2})^2_{J=2}\ (6s_{1/2}\ 6d_{3/2})_{J=2}$	$6s_{1/2}\ (6p_{3/2})^2_{J=2}$	5/2	sp^2 $^2D_{5/2}$	17.713	Not observed
II.G	$(6p_{3/2})^2_{J=2}\ (6s_{1/2}\ 6d_{5/2})_{J=2}$		3/2	sp^2 $^2D_{3/2}$	18.443	Not observed

a. Ref. 9. b. Also borrows intensity from the main line at 14.59 eV.

0 0 0 0 4 2 0 6 3 0 2

Table III. Inelastic loss peaks observed in neutral Pb.

Peak	Transition from the ground state	Relative intensity[a]	Excitation energy, eV[b]	Energy from optical data, eV[c]
0	$6s^2 6p^2\ {}^3P_0$ [d]	---	---	---
1	$6s^2 6p^2\ {}^3P_1$	1	0.97 (1)	0.969
2	$6s^2 6p^2\ {}^3P_2$	4 ± 0.5	1.32 (1)	1.320
3	$6s^2 6p({}^2P_{1/2})7s\ {}^3P_1^{\,o}$	4 ± 0.5	4.37 (1)	4.374
4	$6s^2 6p({}^2P_{1/2})6d \begin{cases} {}^3D_2^{\,o} \\ {}^3D_1^{\,o} \end{cases}$	4 ± 0.5	5.71 (1)	$\begin{cases} 5.709 \\ 5.710 \end{cases}$
5	$6s6p^2$ [e]	16 ± 1	10.52 (2)	---

a. Areas divided by their kinetic energies, relative to peak 1.

b. Values given are averages of two runs. The Pb^+ lines from Table I are used for energy calibration.

c. Ref. 9.

d. Zero loss line (i.e., the main peak).

e. Assignment is tentative as explained in the text.

0 0 0 0 4 2 0 6 3 0 3

FIGURE CAPTIONS

Fig. 1. Schematics of the oven and the ionization chamber used in the present work.

Fig. 2. Photoemission spectrum of Pb vapor at 715°C using 21.21 eV HeI radiation. Lines marked HI and OI arise respectively from HI 10.199 eV and OI 9.493 eV radiation.

Fig. 3. Photoemission spectrum of Pb vapor at 765°C using 21.21 eV HeI radiation.

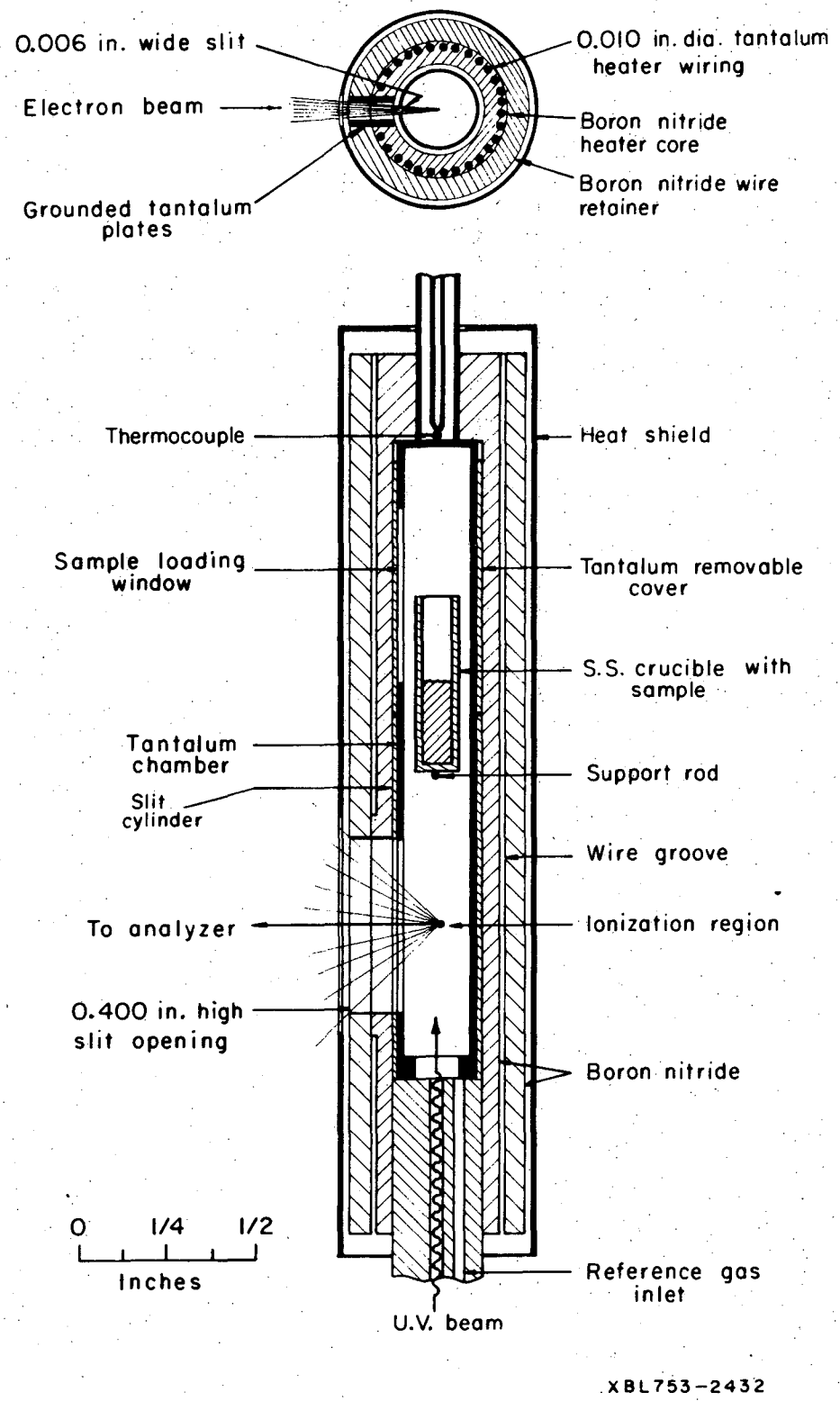
0.006 in. wide slit
Electron beam
Grounded tantalum plates
0.010 in. dia. tantalum heater wiring
Boron nitride heater core
Boron nitride wire retainer
Thermocouple
Heat shield
Sample loading window
Tantalum removable cover
S.S. crucible with sample
Tantalum chamber
Support rod
Slit cylinder
Wire groove
To analyzer
Ionization region
0.400 in. high slit opening
Boron nitride
0 1/4 1/2
Inches
Reference gas inlet
U.V. beam
XBL753-2432

Fig. 1

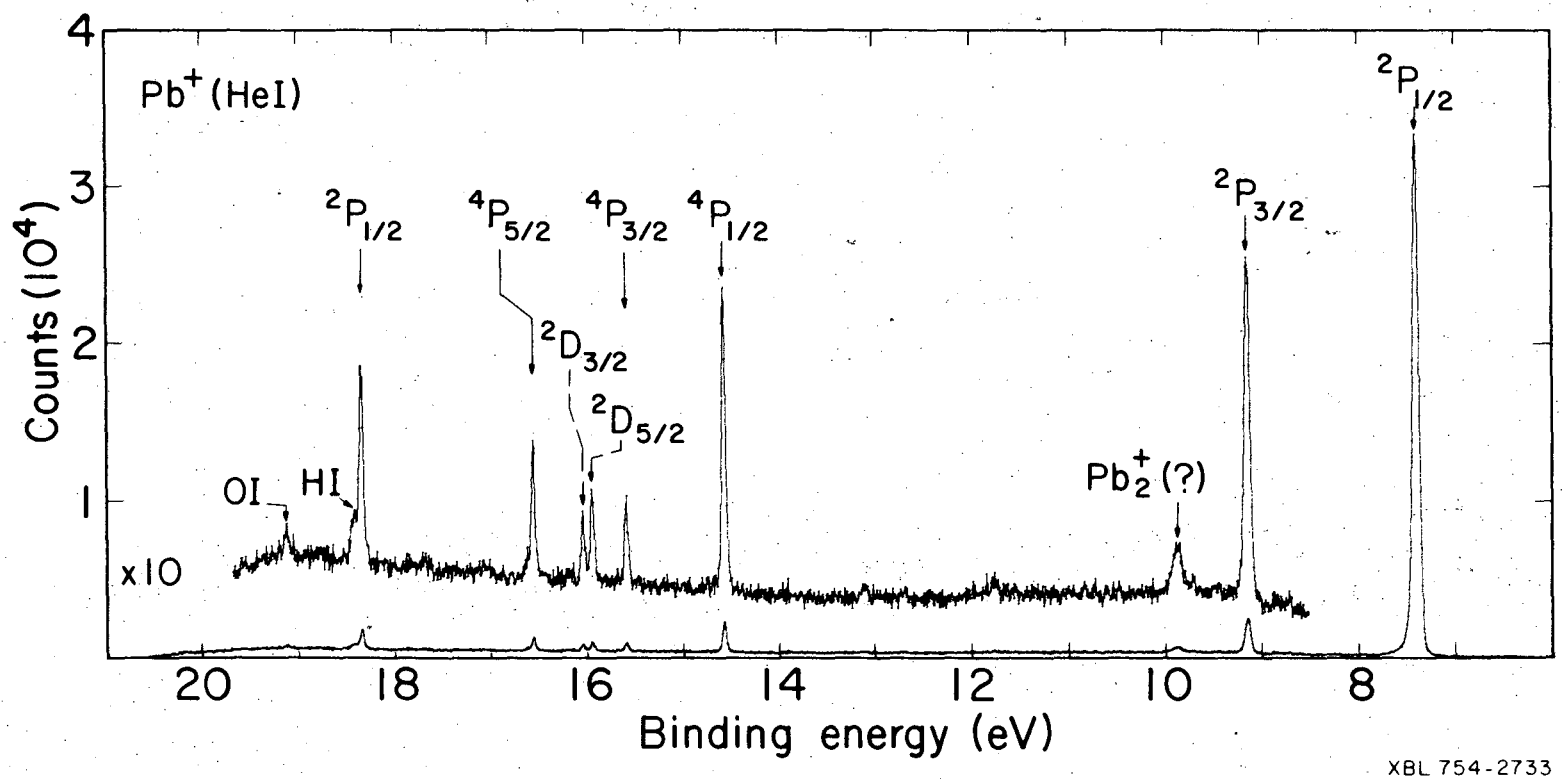
Pb+ (HeI)
Counts (10^4)
4
3
2
1
x10
OI
HI
2P1/2
4P5/2
2D3/2
2D5/2
4P3/2
4P1/2
Pb2+ (?)
2P3/2
2P1/2
20
18
16
14
12
10
8
Binding energy (eV)
XBL 754-2733

Fig. 2

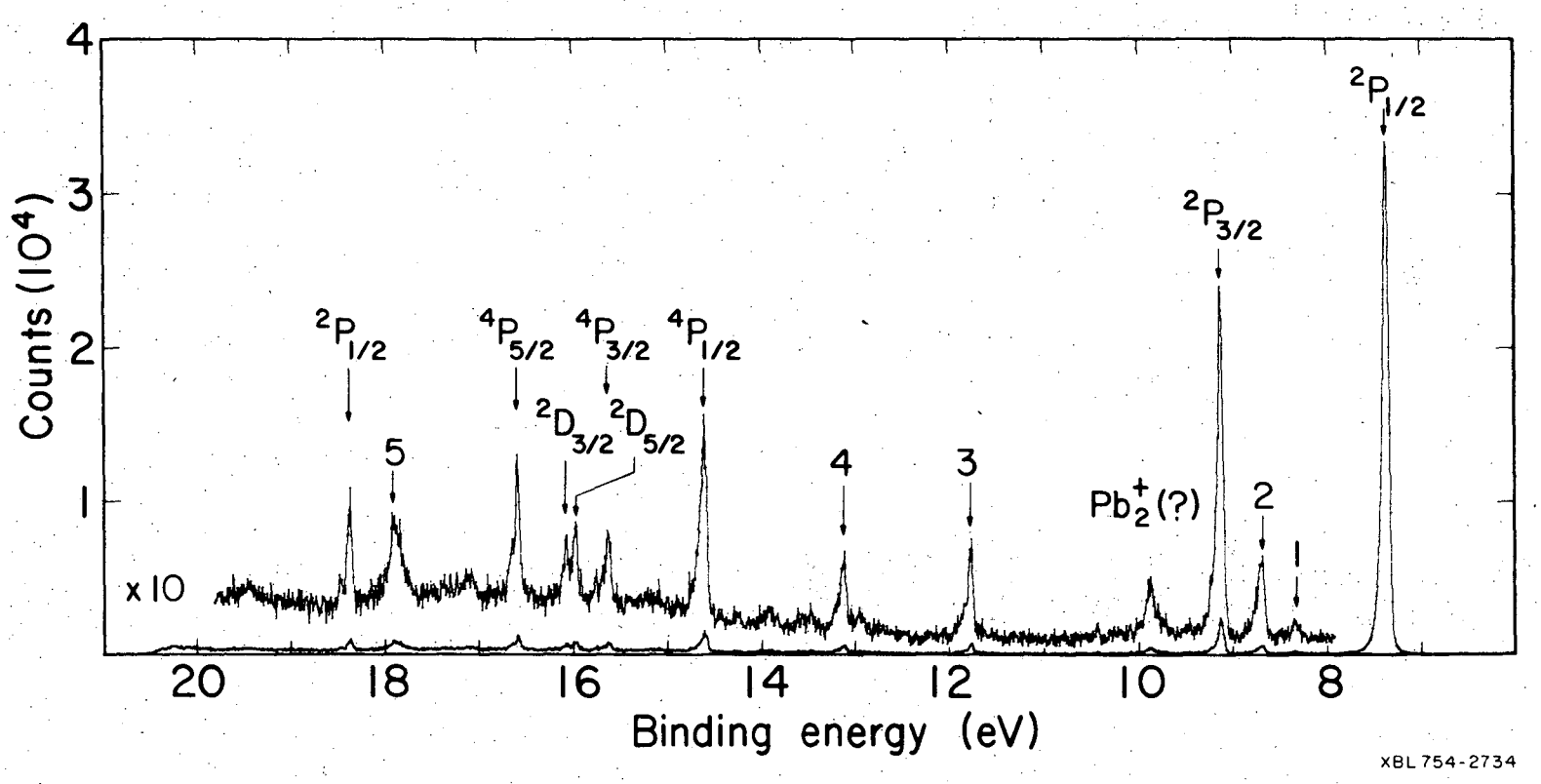
Counts (10^4)
4
3
2
1
x 10
$^2P_{1/2}$
5
$^4P_{5/2}$
$^2D_{3/2}$
$^4P_{3/2}$
$^2D_{5/2}$
$^4P_{1/2}$
4
3
Pb_2^+(?)
$^2P_{3/2}$
2
1
$^2P_{1/2}$
20
18
16
14
12
10
8
Binding energy (eV)
XBL 754-2734

Fig. 3

0 0 0 0 4 2 0 6 3 0 5

LEGAL NOTICE

This report was prepared as an account of work sponsored by the United States Government. Neither the United States nor the United States Energy Research and Development Administration, nor any of their employees, nor any of their contractors, subcontractors, or their employees, makes any warranty, express or implied, or assumes any legal liability or responsibility for the accuracy, completeness or usefulness of any information, apparatus, product or process disclosed, or represents that its use would not infringe privately owned rights.

TECHNICAL INFORMATION DIVISION
LAWRENCE BERKELEY LABORATORY
UNIVERSITY OF CALIFORNIA
BERKELEY, CALIFORNIA 94720